BMB
Reports

BMB Rep. 2022; 55(12): 633-638
www.bmbreports.org

Mettl14 mutation restrains liver regeneration by attenuating mitogens derived from non-parenchymal liver cells

Insook Yang[1], Seung Yeon Oh[2], Suin Jang[2], Il Yong Kim[1,2], You Me Sung[2] & Je Kyung Seong[1,2,3,]*

[1]Laboratory of Developmental Biology and Genomics, College of Veterinary Medicine, Seoul National University, Seoul 08826, [2]Korea Mouse Phenotyping Center (KMPC), Seoul National University, Seoul 08826, [3]Interdisciplinary Program for Bioinformatics and BIO-MAX Institute, Seoul National University, Seoul 08826, Korea

Liver regeneration is a well-known systemic homeostatic phenomenon. The N^6-methyladenosine (m^6A) modification pathway has been associated with liver regeneration and hepatocellular carcinoma. m^6A methyltransferases, such as methyltransferase 3 (METTL3) and methyltransferase 14 (METTL14), are involved in the hepatocyte-specific-regenerative pathway. To illustrate the role of METTL14, secreted from non-parenchymal liver cells, in the initiation phase of liver regeneration, we performed 70% partial hepatectomy (PH) in *Mettl14* heterozygous (HET) and wild-type (WT) mice. Next, we analyzed the ratio of liver weight to body weight and the expression of mitogenic stimulators derived from non-parenchymal liver cells. Furthermore, we evaluated the expression of cell cycle-related genes and the hepatocyte proliferation rate via MKI67-immunostaining. During regeneration after PH, the weight ratio was lower in *Mettl14* HET mice compared to WT mice. The expressions of hepatocyte growth factor (HGF) and tumor necrosis factor (TNF)-α, mitogens derived from non-parenchymal liver cells that stimulate the cell cycle, as well as the expressions of cyclin B1 and D1, which regulate the cell cycle, and the number of MKI67-positive cells, which indicate proliferative hepatocyte in the late G1-M phase, were significantly reduced in *Mettl14* HET mice 72 h after PH. Our findings demonstrate that global *Mettl14* mutation may interrupt the homeostasis of liver regeneration after an acute injury like PH by restraining certain mitogens, such as HGF and TNF-α, derived from sinusoidal endothelial cells, stellate cells, and Kupffer cells. These results provide new insights into the role of METTL14 in the clinical treatment strategies of liver disease. [BMB Reports 2022; 55(12): 633-638]

*Corresponding author. Tel: +82-2-885-8395; Fax: +82-2-885-8397; E-mail: snumouse@snu.ac.kr

https://doi.org/10.5483/BMBRep.2022.55.12.140

Received 13 September 2022, Revised 10 October 2022, Accepted 24 October 2022

Keywords: 70% partial hepatectomy, Hepatocyte growth factor, Liver regeneration, *Mettl14*-knockkout heterozygous mice, Non-parenchymal liver cells

INTRODUCTION

The liver is a solid organ with the regenerative ability to maintain a liver weight to body weight ratio of 100% to meet metabolic demands and regulate homeostasis in the body (1, 2). Therefore, this regenerative ability of the liver renders it a useful model for biochemical, genetic, and bioengineering studies aiming to identify molecular mechanisms underlying liver diseases and improve medical care (2). Extracellular and intracellular factors are involved in the molecular mechanisms underlying liver regeneration (3). Several upstream signaling pathways as well as the detailed transcriptional regulators of liver regeneration have been extensively studied (2).

The m^6A modification pathway has been associated with hepatocellular carcinoma and liver regeneration (4-8). Moreover, it has been revealed to be associated with pathological phenomena such as stem cell differentiation, immunoregulation, and carcinogenesis, and physiological phenomena such as spermatogenesis and adipogenesis (9-13). m^6A is the most common intrinsic RNA modification of eukaryotic cells, and is the most prevalent, abundant, and conserved internal transcriptional modification in eukaryotic cells (7, 14, 15). m^6A is modified by m^6A methyltransferases (writers), such as METTL3 and METTL14, and removed by demethylases (erasers), including FTO and ALKBH5. m^6A is recognized by YTHDF and YTHDC, which are m^6A-binding proteins, also known as "readers" (7). It has been proven to affect liver regeneration in mice lacking hepatocyte-specific m^6A methyltransferase, but its precise role in the initiation phase of liver regeneration that is influenced by endothelial cells, stellate cells, and Kupffer cells, which act as regenerative stimulators, remains to be elucidated (5, 6, 16).

To study this pathway, we performed 70% partial hepatectomy (PH) in mice. This method is the most obvious and well-known experimental technique to induce compensatory regeneration (1). It also helps to observe time-dependent changes in histological and biochemical events in a relatively short period (3, 17). During postoperative liver regeneration, mitogenic stimulators including growth factors, such as hepatocyte growth factor (HGF) and epidermal growth factor (EGF), cytokines, such as TNF-α, IL6, and hormones, such as insulin and norepinephrine, all participate in the proliferative processes (16-21).

ISSN: 1976-670X (electronic edition)

In this study, we generated global *Mettl14* knockout mice to evaluate METTL14-related m^{6}A modification to the non-parenchymal mitogenic pathway in liver regeneration.

RESULTS

m^{6}A modification pathway influences liver regeneration in C57BL/6 mice following 70% PH

To study the m^{6}A modification pathway on liver after surgery, we performed 70% PH according to a published protocol in C57BL/6 mice (22-24). We assessed liver regeneration by measuring the ratio of liver weight to body weight for 7 days after PH. We found a significantly increased ratio which reached 86% of the pre-surgical liver mass within 7 days after PH (Fig. 1A). Next, we assessed the expression of the m^{6}A modification-related proteins METTL3, YTHDF2, and METTL14, and also assessed HGF which is known to regulate liver regeneration (21). Expression of HGF, METTL3 and YTHDF2 increased from 24 h after PH and then gradually decreased from 72 h after PH (Fig. 1B). Expression of METTL14 was gradually increased from 48 h to 7 days after PH (Fig. 1C, D).

To determine the role of the m^{6}A methyltransferases, *Mettl3* and *Mettl14*, we analyzed m^{6}A relative quantification in total RNA at 48 h and 72 h after PH. m^{6}A was significantly increased (Fig. 1E). The global m^{6}A levels measured by m^{6}A colorimetric analysis were gradually increased during liver regeneration (4). These findings are consistent with previous reports and suggest that the m^{6}A modification pathway with METTL3 and METTL14 may influence liver regeneration after PH (5, 6).

Mettl14 depletion attenuates the initiative pathway of liver regeneration after PH in mice

Our results suggested that *Mettl14* is more significantly expressed during liver regeneration after PH; therefore, to validate the effect of METTL14 in the initial pathway of liver regeneration after PH, we produced *Mettl14* knockout mice. To confirm the effect of METTL14 in liver regeneration, we performed 70% PH in *Mettl14* HET mice instead of homozygous mice, which have an embryo-lethal effect, and WT mice (Fig. 2E, F). First, we evaluated the regenerative ability of the liver by calculating the ratio of liver weight to body weight for 72 h after PH. Although hepatic parenchymal proliferation after PH persists for 7 days, we focused on the initiative pathway and cell cycle-related factors (25). The weight ratio was dramatically increased in WT mice than in HET mice from 24 h to 72 h after PH (Fig. 2A). The level of alanine aminotransferase (ALT), a biomarker of liver function, was increased 48 h after PH and recovered close to the pre-surgical level at 72 h after PH in both mice (Fig. 2B). Next, we analyzed the liver regeneration initiative factors, such as HGF, which is a complete growth factor, and TNF-α, which is a cytokine. The mRNA expressions of both HGF and TNF-α were higher in WT mice than in HET mice before surgery and at 72 h after PH (Fig. 2C, D). Furthermore, protein expressions of HGF and TNF-α were reduced at indicated timepoints after PH in HET mice compared to the WT mice (Fig. 2F). Meanwhile, protein expression of EGFR, which is mainly involved in liver regeneration, was increased in HET mice compared to WT mice at 24 h after PH (Fig. 2F) (21).

Mettl14 depletion downregulates cell cycle progression and reduces hepatocyte proliferation

To evaluate the effect of Mettl14 on the cell cycle progression during liver regeneration after PH, we studied the cell cycle-related cyclins B1 and D1, and CDK4 (26). Cyclin D1 plays an important factor in growth and proliferation and is the most

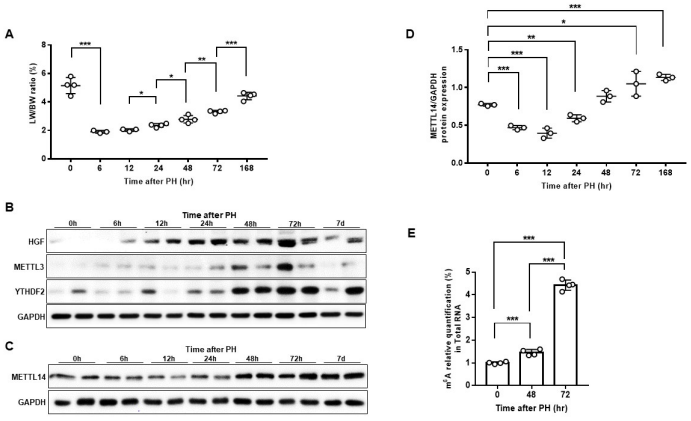

Fig. 1. m^{6}A modification pathway influences on liver regeneration through 70% partial hepatectomy (PH) in C57BL/6 mice. (A) Liver to body weight ratios at the indicated time points after PH in mice (n = 4, each). (B) Representative western blot of HGF, METTL3, YTHDF2 protein levels in the liver at the indicated time points after PH. (C, D) Representative western blot and relative protein level of METTL14 in the liver at the indicated time points after PH. (E) m^{6}A relative quantification ratio in total RNA in the liver after PH. *P < 0.05; **P < 0.01; ***P < 0.001; Error bar represents mean ± SD.

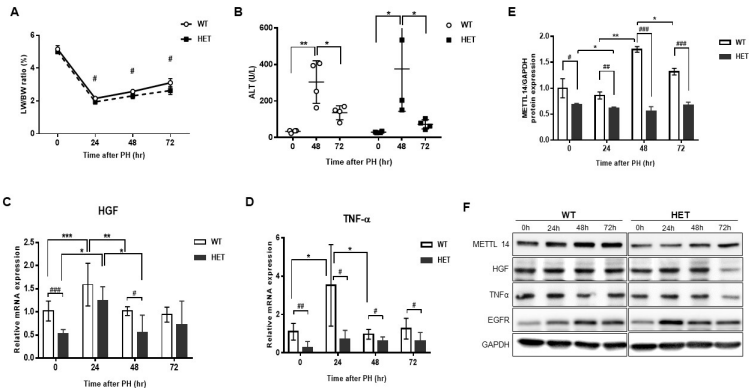

Fig. 2. METTL14 depletion attenuates the initiative pathway of liver regeneration after PH. (A) Liver to body weight ratios at the indicated time points after PH in WT and HET mice (n = 4, each). (B) Serum ALT at the indicated time points after PH in WT and HET mice (n = 4, each). (C, D) HGF and TNF-α mRNA expression levels in the liver at the indicated time points after PH in WT and HET mice (n = 4, each). (E) Relative protein level of METTL14 in the liver at the indicated time points after PH in WT and HET mice (n = 3, each). (F) Representative western blot of METTL14, HGF, TGF-α and EGFR in the liver at the indicated time points after PH in WT and HET mice (n = 3, each). *P < 0.05, **P < 0.01 and ***P<0.001 when compared among time points in same group; $^{\#}$P < 0.05, $^{\#\#}$P < 0.01 and $^{\#\#\#}$P < 0.001 when compared between WT and HET mice; Error bar represents mean ± SD.

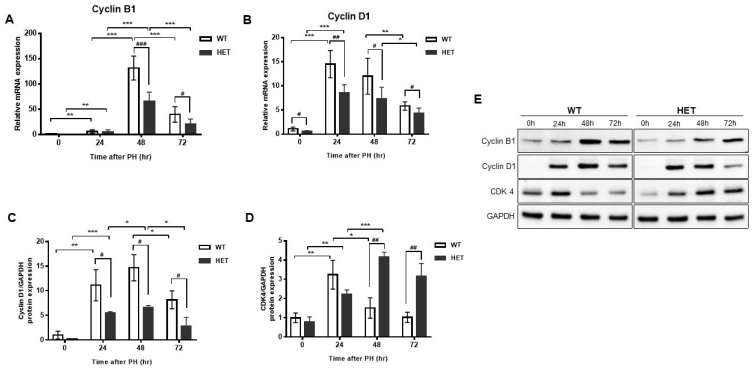

Fig. 3. METTL14 depletion downregulates cell cycle progression in liver regeneration after PH. (A, B) Cyclin B1 and cyclin D1 mRNA expression levels in the liver at the indicated time points after PH in WT and HET mice (n = 4, each). (C, D) Relative protein level of cyclin D1 and CDK4 in the liver at the indicated time points after PH in WT and HET mice (n = 3, each). (E) Representative western blot of cyclin B1, cyclin D1 and CDK4 in the liver at the indicated time points after PH in WT and HET mice. *P < 0.05, **P < 0.01 and ***P < 0.001 when compared among time points in same group; $^{\#}$P < 0.05, $^{\#\#}$P < 0.01 and $^{\#\#\#}$P < 0.001 when compared between WT and HET mice; Error bar represents mean ± SD.

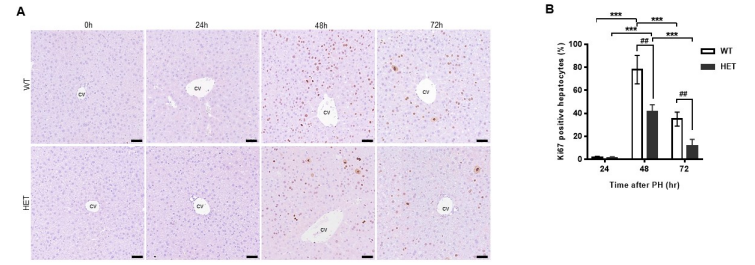

Fig. 4. METTL14 depletion reduces hepatocyte proliferation in liver regeneration after PH. (A) Representative immunohistochemical images showing MKI67 staining at the indicated time points after PH. (B) Quantification of MKI67 staining in hepatocyte nuclei at the indicated time points after PH (n = 4, each). ***P < 0.001 when compared among time points in same group; $^{\#\#}$P < 0.01 when compared between WT and HET group; Error bar represents mean ± SD.; Scale bar = 50 μm.

reliable marker for G1 phase progression in liver regeneration (27). CDK4 is a cyclin-dependent kinase and the main regulator of the cell cycle; it can combine with cyclin D1 (28). Cyclin B1 is related to the M phase (27). The mRNA and protein expression of cyclin B1 and cyclin D1 at 24-72 h after PH were higher in WT mice than in HET mice (Fig. 3A-C, E). However, CDK4 protein expression was not consistent with that of cyclin D1 (Fig. 3D, E). As shown in Fig. 3, although the time-dependent results in mRNA and protein expression levels during liver regeneration did not follow the same pattern, there were similarities in the trends that increased and gradually decreased.

Lastly, we analyzed the hepatocyte proliferation rate using immunostaining of MKI67, which is more abundant in DNA synthesis and mitosis than in the early or even the very late G1 phase, as an indicator of cell cycle progression (29). The proliferation rate was calculated by the number of stained nuclei (Fig. 4A). The rate of MKI67-positive hepatocytes was significantly increased in WT mice than in HET mice at 48 h and 72 h after PH (Fig. 4B).

DISCUSSION

It is well known that the liver has a distinctive and dynamic ability to recover its original size to maintain body homeostasis (1). METTL14 has an important role in endogenous RNA modification as an m^6A methyltransferase (7). A recent study has shown that METTL14 is involved in liver regeneration following acute injuries, such as PH (6).

The regeneration process after PH is influenced by extensive interaction of parenchymal as well as non-parenchymal cells. The influence of the METTL14-related m^6A modification pathway on non-parenchymal cells, such as sinusoidal endothelial cells, stellate cells, and Kupffer cells, is not yet understood. In this study, we performed surgical experiments using HET mice, to evaluate the influence of METTL14 on liver regeneration mediated by non-parenchymal liver cells. We found that the liver mass was similar in both the HET and WT mice over 8 weeks of age, as measured by the ratio of their liver weight to body weight (Fig. 2A). Our findings supported previous findings by Cao *et al*. (6) showing liver development in mice with liver-specific Mettl14 knockout was similar to that in wild type mice. However, to confirm whether the liver development in the *Mettl14*-knockout heterozygous mice we used is normal, more research is required. Meanwhile, the ratio of liver weight to body weight between 24 h and 72 h after PH was significantly decreased in HET mice compared to WT mice. Furthermore, mRNA expression of HGF, which is a complete mitogen secreted by stellate cells, was down-regulated in HET mice compared to WT mice. Furthermore, mRNA expression of TNF-α, which is a mitogen released by endothelial cells and Kupffer cells, was significantly decreased in HET mice than in WT mice at 72 h after PH. This experiment focused on the findings at 72 h after PH, as most of the active postoperative hepatocellular proliferation occurs during this period (25, 30). Protein expression of these two mitogens was notably reduced at 72 h after PH in HET mice compared to WT mice. These results support the hypothesis that METTL14-mediated m^6A modification can affect the expression of certain mitogens derived from non-parenchymal liver cells, leading to the initiation phase of liver regeneration. In contrast, the protein expression of EGFR was increased at 24 h after PH in HET mice compared to WT mice. EGFR is a membrane receptor that binds to EGF, which is one of the complete mitogens secreted from the Brunner's gland of the duodenum (3, 26). This implies that specific growth factors which originate from organs besides the liver are not influenced by the m^6A modification pathway. Subsequently, we analyzed the cell-cycle pathway, which is stimulated by HGF and TNF-α. The expression of cyclin D1, which is a major regulator of the G1 phase, was downregulated in HET mice compared to the WT mice and was particularly remarkably decreased at 72 h after PH. In addition, the expression of cyclinB1, which is a regulator of the mitosis phase, decreased faster in HET mice than in WT mice. These consistent cascading results suggest that the cell cycle is decreased in HET mice. CDK4 is a transcription factor of the G1 phase. Our findings revealed that there was a tendency toward upregulation of CDK4 expression in HET mice, unlike that of cell cyclins. This suggests the presence of a compensatory response, which is not affected by METTL14-mediated m^6A modification. However, further research is needed to validate our findings. Finally, we analyzed the hepatocyte proliferation rate using MKI67-positive hepatocytes, which was significantly decreased in HET mice compared to WT mice, and consistent with the results of the liver weight-to-body weight ratio. In this experiment, we found that novel biological events involving mitogenic pathways, induced by non-parenchymal liver cells, are disturbed by incomplete *Mettl14* expression. Nonetheless, it remains a challenge to prove that HGF and TNF-α are actual targets of *Mettl14* by assessing their RNA transcripts for m^6A enrichment. We believe that additional research into the relationship of non-parenchymal liver cells using conditional *Mettl14* knockout mice will help us overcome the limitations of our work.

Taken together, this study suggested that the m^6A modification pathway is essential in compensatory liver regeneration involving non-parenchymal liver cells after acute injury. Furthermore, these results provide new insights into the existing knowledge on the regenerative processes in the liver following surgical treatment.

MATERIALS AND METHODS

Animals

C57BL/6 mice purchased from the Korea Research Institute of Bioscience and Biotechnology (KRIBB) were used for all experiments in this study. Mice were maintained under a 12-h light-dark cycle and were provided with free access to water

and a regular chow diet in a specific pathogen-free (SPF) facility.

The C57BL/6N-Mettl14<em1(IMPC)Tcp> mice were produced as part of the KOMP2-Phase2project at the Center for Phenogenomics of International Mouse Phenotyping Consortium (IMPC) and were obtained from the Canadian Mouse Mutant Repository. According to IMPC data, Homozygous offspring of *Mettl14* knockout mice exhibited preweaning or embryonic lethality.

The *Mettl14* HET mice and WT mice were created by the deletion of *Mettl14*; endonuclease-mediated 1 allele, as published by the IMPC. Genotyping was performed using genomic DNA desolated from tails according to the IMPC screening protocol.

Partial hepatectomy

Male mice, aged 8 to 10 weeks, were subjected to 70% partial hepatectomy under isoflurane (Hana Pharm Co., Ltd.) inhalation anesthesia according to a published protocol (22-24).

The left lateral and median lobe of the liver along with the gall bladder were ligated and removed. The gall bladder was always removed during surgery to avoid damage. For postoperative care, all animals were administrated 5 mg/kg ketoprofen (Daehan Inc., Korea) intraperitoneally to control pain (24). All mice were sacrificed at the indicated time. The weight of the remnant livers was measured, which were then subsequently fixed in 4% paraformaldehyde and snap-frozen in liquid nitrogen immediately after extraction. Animal experiments were performed following the "Guide for Animal Experiments" edited by the Korean Academy of Medical Sciences and "ARRIVE Guidelines" by NC3Rs and approved by the Institutional Animal Care and Use Committee of Seoul National University, Seoul, Korea (IACUC approval no. SNU-190919-9, SNU-210709-4).

m^6A quantification

The m^6A level in total RNA in the liver tissues was assessed using the EpiQuikTM m^6A RNA Methylation Quantification Kit (cat. P-9005; Epigentek Group Inc., USA) following the manufacturer's protocol. Total RNA (200 ng) was added to each well, followed by the addition of the capture antibody solution and detection antibody solution (31). The absorbance at 450 nm was colorimetrically measured to determine the m^6A level.

Histology and Immunohistochemistry

Liver tissues were fixed overnight in 4% paraformaldehyde, embedded in paraffin, and used for hematoxylin and eosin (H&E) staining, as well as immunostaining with antibodies against MKI67 (cat. ab16667; Abcam, Cambridge, UK). For immunostaining, the slides containing tissue sections were first heated in citrate buffer for antigen retrieval before being treated with horse serum for blocking the endogenous peroxidase activity. Slides were then incubated with the primary antibody overnight, followed by a 30 min incubation with the secondary antibody (horse Anti Rabbit HRP). The slides were then developed with diaminobenzidine (DAB). To quantify hepatocyte proliferation, ten fields per slide were randomly chosen under the microscope after immunostaining to count MKI67-positive hepatocytes and the percentage of MKI67-positive hepatocytes was calculated against the total hepatocytes in the fields.

Western blotting

Protein lysates were prepared in RIPA buffer containing 0.5 mM phenylmethane sulfonyl fluoride (PMSF), 4 μg/ml leupeptin, 4 μg/ml aprotinin, and 4 μg/ml pepstatin, separated by sodium dodecyl sulfate (SDS)-polyacrylamide gel electrophoresis (PAGE), and transferred to polyvinylidene fluoride (PVDF) membranes. Membranes were incubated with the following primary antibodies overnight: METTL3 (cat. 96391, Cell Signaling Technology, MA, USA), METTL14 (cat. HAP038002; Sigma-Aldrich, MO, USA), YTHDF2 (cat. ab220163), TNF-α (cat. 11948, Cell Signaling Technology), HGF (cat. ab83760), EGFR (cat. 2646; Cell Signaling Technology), Cyclin B1 (cat. 12231; Cell Signaling Technology), Cyclin D1 (cat. 2978; Cell Signaling Technology), CDK4 (cat. Sc-23896; Santa Cruz Biotechnology, Inc., USA), GAPDH (cat. 2118, Cell Signaling Technology) then incubated with the secondary antibody goat-anti-rabbit-HRP or goat-anti-mouse-HRP for 1 h. Antibody binding was visualized using the Pierce TM ECL western blotting detection system (Chemi-Doc XRS+System; Bio-rad, CA, USA).

mRNA isolation and real-time polymerase chain reaction (RT-PCR)

Total RNA was isolated from the liver using Trizol (Ambion, TX, USA) reagent. RT-PCR analysis of the isolated mRNA was performed in a two-step reaction (32). In the first step, a complementary DNA strand was synthesized using the Acculower RT reverse transcription kit (Bioneer, Daejeon, South Korea), and the second step was performed on a 7500 Real-Time PCR System (Applied Biosystems, MA, USA) with SYBR green (BIO-94020; Bioline, Toronto, Canada) and specific primers for each of the target genes. Each assay included the *36B4* gene as an endogenous reference. Gene expression was calculated using the $2^{-\Delta\Delta CT}$ method.

Statistical analysis

Statistical analysis was performed using GraphPad Prism 4 (GraphPad Software, http://www.graphpad.com). Data are presented as mean ± standard deviation (SD). Statistical significance among more than two groups was assessed using Student's t-test. A P-value less than 0.05 was considered statistically significant.

ACKNOWLEDGEMENTS

This research was supported by Korea Mouse Phenotyping Project (2013M3A9D5072550) of the National Research Foundation funded by the Ministry of Science and ICT (2012M 3A9D1054622) and partially supported by the Brain Korea 21 Plus Program and the Research Institute for Veterinary Science of Seoul National University.

CONFLICTS OF INTEREST

The authors have no conflicting interests.

REFERENCES

1. Michalopoulos GK (2021) Novel insights into liver homeostasis and regeneration. Nat Rev Gastroenterol Hepatol 18, 369-370
2. Kurinna S and Barton MC (2011) Cascades of transcription regulation during liver regeneration. Int J Biochem Cell Biol 43, 189-197
3. Michalopoulos GK (2013) Principles of liver regeneration and growth homeostasis. Compr Physiol 3, 485-513
4. Ma JZ, Yang F, Zhou CC et al (2017) METTL14 suppresses the metastatic potential of hepatocellular carcinoma by modulating N^6-methyladenosine-dependent primary MicroRNA processing. Hepatology 65, 529-543
5. Meng J, Zhao Z, Xi Z et al (2022) Liver-specific Mettl3 ablation delays liver regeneration in mice. Genes Dis 9, 697-704
6. Cao X, Shu Y, Chen Y et al (2021) Mettl14-mediated m^6a modification facilitates liver regeneration by maintaining endoplasmic reticulum homeostasis. Cell Mol Gastroenterol Hepatol 12, 633-651
7. Jiang X, Liu B, Nie Z et al (2021) The role of m6A modification in the biological functions and diseases. Signal Transduct Target Ther 6, 74
8. Lu J, Qian J, Yin S et al (2020) Mechanisms of RNA N^6-methyladenosine in hepatocellular carcinoma: from the perspectives of etiology. Front Oncol 10, 1105
9. Lin S and Gregory RI (2014) Methyltransferases modulate RNA stability in embryonic stem cells. Nat Cell Biol 16, 129-131
10. Shulman Z and Stern-Ginossar N (2020) The RNA modification N^6-methyladenosine as a novel regulator of the immune system. Nat Immunol 21, 501-512
11. Hua W, Zhao Y, Jin X et al (2018) METTL3 promotes ovarian carcinoma growth and invasion through the regulation of AXL translation and epithelial to mesenchymal transition. Gynecol Oncol 151, 356-365
12. Yang X, Zhang S, He C et al (2020) METTL14 suppresses proliferation and metastasis of colorectal cancer by down-regulating oncogenic long non-coding RNA XIST. Mol Cancer 19, 46
13. Lin Z, Hsu PJ, Xing X et al (2017) Mettl3-/Mettl14-mediated mRNA N^6-methyladenosine modulates murine spermatogenesis. Cell Res 27, 1216-1230
14. Fu Y, Dominissini D, Rechavi G et al (2014) Gene expression regulation mediated through reversible m^6A RNA methylation. Nat Rev Genet 15, 293-306
15. Jia G, Fu Y and He C (2013) Reversible RNA adenosine methylation in biological regulation. Trends Genet 29, 108-115
16. Malik R and Hodgson H (2002) The relationship between the thyroid gland and the liver. QJM 95, 559-569
17. Fausto N, Campbell JS and Riehle KJ (2006) Liver regeneration. Hepatology 43, S45-53
18. Akerman P, Cote P, Yang SQ et al (1992) Antibodies to tumor necrosis factor-alpha inhibit liver regeneration after partial hepatectomy. Am J Physiol Gastrointest Liver Physiol 263, G579-G585
19. Cressman DE, Greenbaum LE, DeAngelis RA et al (1996) Liver failure and defective hepatocyte regeneration in interleukin-6-deficient mice. Science 274, 1379-1383
20. Cruise JL, Houck KA and Michalopoulos GK (1985) Induction of DNA synthesis in cultured rat hepatocytes through stimulation of α1 adrenoreceptor by norepinephrine. Science 227, 749-751
21. Michalopoulos GK and DeFrances M (2005) Liver regeneration. Adv Biochem Eng Biotechnol 93, 101-134
22. Higgins GM and Anderson RM (1931) Experimental pathology of the liver. I. Restoration of the white rat following partial surgical removal. Arch Path 12, 186-202
23. Mitchell C and Willenbring H (2008) A reproducible and well-tolerated method for 2/3 partial hepatectomy in mice. Nat Protoc 3, 1167-1170
24. Yang I, Son Y, Shin JH et al (2022) Ahnak depletion accelerates liver regeneration by modulating the TGF-beta/Smad signaling pathway. BMB Rep 55, 401-406
25. Michalopoulos GK (2007) Liver regeneration. J Cell Physiol 213, 286-300
26. Olsen PS, Poulsen SS and Kirkegaard P (1985) Adrenergic effects on secretion of epidermal growth factor from Brunner's glands. Gut 26, 920-927
27. Fausto N (2000) Liver regeneration. J Hepatol 32, 19-31
28. Mullany LK, White P, Hanse EA et al (2008) Distinct proliferative and transcriptional effects of the D-type cyclins in vivo. Cell Cycle 7, 2215-2224
29. Gerlach C, Sakkab DY, Scholzen T et al (1997) Ki-67 expression during rat liver regeneration after partial hepatectomy. Hepatology 26, 573-578
30. Marongiu F, Marongiu M, Contini A et al (2017) Hyperplasia vs hypertrophy in tissue regeneration after extensive liver resection. World J Gastroenterol 23, 1764-1770
31. Li J, Zhu L, Shi Y et al (2019) m6A demethylase FTO promotes hepatocellular carcinoma tumorigenesis via mediating PKM2 demethylation. Am J Transl Res 11, 6084-6092
32. Kim YJ, Kim HJ, Lee WJ et al (2020) A comparison of the metabolic effects of treadmill and wheel running exercise in mouse model. Lab Anim Res 36, 3